# Rethinking the application of the first nucleation theorem to particle formation

Hanna Vehkamäki, Matthew J. McGrath, Theo Kurtén, Jan Julin, Kari E. J. Lehtinen et al.

Citation: J. Chem. Phys. **136**, 094107 (2012); doi: 10.1063/1.3689227
View online: http://dx.doi.org/10.1063/1.3689227
View Table of Contents: http://jcp.aip.org/resource/1/JCPSA6/v136/i9
Published by the American Institute of Physics.

# Rethinking the application of the first nucleation theorem to particle formation

Hanna Vehkamäki,[1,a)] Matthew J. McGrath,[1,b)] Theo Kurtén,[1,c)] Jan Julin,[1,d)]
Kari E. J. Lehtinen,[2] and Markku Kulmala[1]
[1]*Department of Physics, P.O. Box 64, University of Helsinki, Finland*
[2]*Department of Applied Physics, University of Eastern Finland and Finnish Meteorological Institute, P.O. Box 1627, Kuopio 70211, Finland*

(Received 7 October 2011; accepted 8 February 2012; published online 5 March 2012)

The critical cluster is the threshold size above which a cluster will be more likely to grow than to evaporate. In field and laboratory measurements of new particle formation, the number of molecules of a given species in the critical cluster is commonly taken to be the slope of the log-log plot of the formation rate versus the concentration of the species. This analysis is based on an approximate form of the first nucleation theorem, which is derived with the assumption that there are no minima in the free energy surface prior to the maximum at the critical size. However, many atmospherically relevant systems are likely to exhibit such minima, for example, ions surrounded by condensable vapour molecules or certain combinations of acids and bases. We have solved numerically the birth-death equations for both an electrically neutral one-component model system with a local minimum at pre-critical sizes and an ion-induced case. For the ion-induced case, it is verified that the log-log slope of the nucleation rate versus particle concentration plot gives accurately the difference between the cluster sizes at the free energy maximum and minimum, as is expected from the classical form of the ion-induced nucleation rate. However, the results show that applying the nucleation theorem to neutral systems with stable pre-nucleation clusters may lead to erroneous interpretations about the nature of the critical cluster. © *2012 American Institute of Physics*. [http://dx.doi.org/10.1063/1.3689227]

## I. INTRODUCTION

The formation of 1–2 nm sized atmospheric particles from condensable gases is observed in a multitude of locations around the world.[1] Modelling studies estimate that particles formed in the atmosphere constitute 20%−80% of all cloud condensation nuclei,[2–4] making them significant players in atmospheric processes. The formation mechanism and participating vapours have not yet been resolved. A key question concerns the size and composition of the critical cluster, which is the smallest cluster that will grow by condensation without an energetic barrier. In many locations around the world, the concentrations of newly born particles correlate well with some power of the gas-phase sulphuric acid concentration.[5–8] In search of a molecular understanding of particle formation, scientists have taken the slope of the particle formation rate when plotted against the sulphuric acid concentration on a log-log scale to give the number of sulphuric acid molecules in the critical cluster.[9–13] This analysis is based on the first nucleation theorem, derived for homogeneous and heterogeneous one- and multicomponent nucleation.[14–17] The general form of the theorem involving the formation free energy can easily be converted to use the measurable nucleation rate, assuming that all clusters smaller than the critical size are more likely to decay than grow, and only monomer-cluster collisions and evaporation of monomers (not cluster-cluster collisions and evaporation of larger clusters than monomers) need to be taken into account.

Vapours where the concentrations of dimers and larger clusters are non-negligible compared to the monomer concentration are known as associated vapours. The various associated vapours include substances where dimer and larger cluster concentrations comprise only a few percent of the total concentration, as well as vapours where the total concentration is almost completely dominated by, for example, dimers.[18–21] As the present work concerns vapours with stable pre-nucleation clusters, the conclusions presented are pertinent to situations where the monomer concentration does not dominate. In this case, cluster-cluster collisions and evaporation of non-monomer entities play a significant role.

Even in the case where no stable pre-nucleation clusters exist, the applicability of the nucleation theorem requires constant temperature (and in the multicomponent case constant concentrations of all other vapours as well). Spatial and temporal variation in the vapour concentrations and temperature may also skew the results. Another complication is that the observed formation rate is not actually the nucleation rate $J$ but the formation rate of clusters or particles that reach the detection limit. This may be lower than the nucleation rate due to self-coagulation or coagulation onto pre-existing larger particles, and in laboratory experiments also due to wall losses. These issues, however, deserve separate studies, and are beyond the scope of this work.

[a)]Electronic mail: hanna.vehkamaki@helsinki.fi.
[b)]Also at Department of Biophysics, Graduate School of Science, Kyoto University, Kyoto 606-8502, Japan.
[c)]Also at Copenhagen Centre for Atmospheric Research, Department of Chemistry, University of Copenhagen, Denmark.
[d)]Also at Department of Applied Environmental Science (ITM), Stockholm University, SE-10691 Stockholm, Sweden.

 

## II. MODELS AND METHODS

In a barrierless cluster formation process, a dimer and all subsequent cluster sizes evaporate back to monomers at a lower rate than colliding with (and sticking to) another molecule of the nucleating vapour, and the critical cluster size is nominally $i = 1$. In nucleation, some critical number of molecules $i_{\max} > 1$ is required before all subsequent clusters are more likely to grow than decay. This is manifested as a barrier in the formation free energy surface when plotted against the size of the cluster.[22–24] The stable pre-nucleation clusters express themselves as minima on the free energy surface at sizes smaller than the critical cluster size.

In the atmosphere, the particle formation process is likely to involve several components which vary with location and conditions. For simplicity, we study the effect of free energy minima on the application of the nucleation theorem in a simple one-component system and an ion-induced one-component case. We restrict our study to cases with one minimum at smaller sizes than the maximum corresponding to the critical cluster. Thus, the minimum always lies below the zero level corresponding to the reference size, usually a monomer. We chose simple model systems without direct atmospheric relevance in the interest of proof of concept. In a one-component system, the cluster distributions and the particle formation rate can be accurately solved without numerical problems, and compared to analytical, exact formulae, as well as their approximate versions. This allows us to pinpoint the exact reasons for deviation from customarily expected behaviour. The price of using the simplified system is that the vapour concentrations required for particle formation in our model are far above atmospherically relevant levels. The proof of concept, however, is not hampered by the actual numerical values, and the saturation ratios are actually quite realistic. Using the temperature range 273−298 K, relative humidities 50%−90% and sulphuric acid concentrations $10^5 - 10^8$ cm$^{-3}$, the saturation ratio of sulphuric acid vapour above the liquid solution having the composition of an equilibrium cluster ranges from 1 to 100. To calculate these saturation ratios, we have used the liquid droplet model and thermodynamic data as in Noppel, Vehkamäki, and Kulmala, 2002.[25]

Clusters of a given size are formed by collisions of two smaller clusters as well as the evaporation of larger clusters, and they move to another size when they collide with other clusters or evaporate. In the interest of keeping the system simple, we do not include wall losses or coagulation of the clusters with larger particles, which certainly affect the evolution of the cluster distribution in chamber studies or field observations. The effect of these processes to the application of the nucleation theorem is worth a separate study.

The concentration ($c_i$) of clusters of size $i$ in a one-component system is governed by the birth-death equations

$$\frac{dc_i}{dt} = \sum_{i'<i} \frac{1}{2}\beta_{i',(i-i')}c_{i'}c_{(i-i')} + \sum_{i'} \gamma_{(i+i')\to i}c_{i+i'} - \sum_{i'} \beta_{i,i'}c_i c_{i'} - \sum_{i'<i} \frac{1}{2}\gamma_{i\to i'}c_i, \quad (1)$$

where $\beta_{i,i'}$ is the collision coefficient between the $i$-mer and the $i'$-mer, and $\gamma_{i\to i'}$ is the rate coefficient at which an $i$-mer decays producing an $i'$-mer (and an $(i - i')$-mer). The collision coefficients are taken to be hard sphere collision rates,

$$\beta_{i,i'} = \left(\frac{3}{4\pi}\right)^{1/6}\left(\frac{6kT}{m_i} + \frac{6kT}{m_{i'}}\right)^{1/2}\left(V_i^{1/3} + V_{i'}^{1/3}\right)^2, \quad (2)$$

where $m_i$ and $V_i$ are the mass and volume of the cluster with $i$ molecules. The evaporation coefficients $\gamma_{i\to i'}$ are calculated from the cluster formation free energies $\Delta G_i$ based on detailed balance and the equilibrium cluster distribution $N_i = c_{\text{ref}}\exp(-\Delta G_i/kT)$, resulting in[26,27]

$$\gamma_{i\to i'} = \beta_{(i-i'),i'}N_{i-i'}N_{i'}/N_i. \quad (3)$$

The classical formation free energy of a cluster in homogeneous nucleation is

$$\Delta G_i = -(i-1)kT\ln S + [A_i - A_1]\sigma, \quad (4)$$

where $A_i$ is surface area of the cluster with $i$ molecules, $\sigma$ is the surface tension, and $S$ is the saturation ratio. The formation free energy of a cluster in ion-induced nucleation is

$$\Delta G_i = -ikT\ln S + (A - A_0)\sigma + \frac{q^2}{8\pi\varepsilon_0}\left(1 - \frac{1}{\varepsilon_r}\right)\left(\frac{1}{r_i} - \frac{1}{r_{\text{ion}}}\right), \quad (5)$$

where $r_i$ is the radius of the cluster with $i$ water molecules, $q$ is the charge of the ion, $\epsilon_0$ is the permittivity of vacuum, $\varepsilon_r$ is the dielectric constant of the liquid, and $r_{\text{ion}}(=r_0)$ is the radius of the ion. The formation free energy must be normalised so that for a reference size, whose concentration is $c_{\text{ref}}$, the formation free energy is $\Delta G_{\text{ref}} = 0$. For homogeneous one-component nucleation, the natural choice for the reference size is the monomer ($i = 1$), and thus Eq. (4) is the self-consistent form $\Delta G_i = \Delta G'_i - \Delta G'_1$. For ion-induced nucleation, the bare ion ($i = 0$) is chosen as the reference size. In a steady state, the time derivatives of all cluster concentrations are zero. Typically the monomer concentration $c_1$ is set to a known value, giving rise to a time-independent nucleation rate, that is, the net formation rate of critical clusters. In the case where there are many more monomers than clusters of any other size, only monomer-cluster collisions and the evaporation of single monomers need to be taken into account. In this case, the accurate expression for the steady-state nucleation rate in a one-component system is[26]

$$J_{\text{SUM}} = \left(\sum_i \frac{1}{c_1\beta_{i,1}c_{\text{ref}}\exp\left(\frac{-\Delta G_i}{kT}\right)}\right)^{-1}. \quad (6)$$

The approximate expression for the nucleation rate is

$$J_{\text{approx}} = \frac{1}{S}\beta_{i^*,1}Zc_{\text{ref}}\exp\left(\frac{-\Delta G_{i^*}}{kT}\right) \quad (7)$$

with the saturation ratio defined as $S = c_1kT/p_s$, where $p_s$ is the saturation vapour pressure. $Z$ is the Zeldovich factor given by

$$Z = \sqrt{\frac{\sigma}{kT}}\frac{v_{\text{liquid}}}{2\pi r^{*2}}, \quad (8)$$

where $v_{\text{liquid}}$ is the volume of a single molecule in the liquid and $r^*$ is the critical cluster radius, both of which are calculated using the bulk liquid density. Equation (7) is obtained from the accurate form Eq. (6) by assuming that the formation free energy exhibits no minima and a single maximum. Then, the summation in Eq. (6) can be converted into an integral where only the region of this maximum in $\Delta G_i$ contributes significantly.

The slope of the log-log plot of the rate versus the saturation ratio (or equally the monomer concentration) following from the nucleation rate expression Eq. (6) is[28]

$$\left(\frac{\partial \ln J}{\partial \ln c_1}\right)_T = \left(\frac{\partial \ln J}{\partial \ln S}\right)_T = \frac{\sum_i \frac{i}{c_1 \beta_{i,1} c_{\text{ref}} \exp\left(\frac{-\Delta G_i}{kT}\right)}}{\sum_i \frac{1}{c_1 \beta_{i,1} c_{\text{ref}} \exp\left(\frac{-\Delta G_i}{kT}\right)}} + 1. \tag{9}$$

In a case where the formation free energy exhibits no minima and a single maximum the ratio of sums in the right hand side of Eq. (9) is approximately equal to the critical size[28] giving rise to the familiar form of the first nucleation theorem

$$\left(\frac{\partial \ln J}{\partial \ln c_1}\right)_T = \left(\frac{\partial \ln J}{\partial \ln S}\right)_T = i^* + \epsilon, \tag{10}$$

where $\epsilon$ is a small correction term arising from the kinetic prefactor $\frac{1}{S}\beta_{i^*,1} Z c_{\text{ref}}$ in the expression of the nucleation rate. This form generalises to multicomponent cases.[15] For the one-component case $\epsilon = 1$ and for multicomponent cases $\sum_k \epsilon_k = 1$, where the sum is taken over all components.[29] In the case of heterogeneous nucleation the measured variable is nucleation probability instead of nucleation rate. In this case an adjusted form of the nucleation theorem can be applied.[30–32] Equation (10) follows also from the approximate nucleation rate (7) using the fundamental form of the theorem involving the formation free energy

$$\left(\frac{\partial \Delta G_{i^*}}{\partial \ln c_1}\right)_T = \left(\frac{\partial \Delta G_{i^*}}{\partial \ln S}\right)_T = -i^*. \tag{11}$$

The validity of Eq. (11) is not questioned in our work. $\Delta G_i$ is defined as the difference in free energy between the cluster with $i$ molecules and $i$ single molecules in the vapour. Thus, it is understandable that Eqs. (6)−(10) which involve the rate, work only for processes where monomer addition is the dominant mechanism of cluster formation.

We have solved the birth-death equations numerically for various one-component systems following the time evolution of the cluster distribution until a steady state was established. The differential equations were generated and solved through the use of the atmospheric cluster dynamics code (ACDC),[33] a combination of scripts using the MATLAB program suite and the PERL scripting language. The MATLAB script calculates the solution to the differential equations using the `ode15s` solver, which is recommended for systems of stiff equations. In order to have a fast, flexible, and error-free method of generating these MATLAB scripts, a PERL script was employed. The PERL script allows the addition/removal of collisions and evaporations of non-monomer clusters with a simple command-line switch, as well as changes in the total number of clusters considered and the number of components by making simple alterations to the input file. All of this enables a wide variety of tests to be performed quickly and accurately. The formation rate was computed during the solution of the differential equations by calculating the number of clusters which grow to larger sizes than the system boundary, $i_{\text{boundary}}$. In the case of only monomer evaporations and collisions, this expression is simple, as the only way a cluster can grow larger than the clusters included in the system is if a monomer collides with the largest cluster whose concentration is being calculated. In other words, in a single component system of 100 equations, the rate is given by

$$J_{\text{ACDC}} = \beta_{100,1} c_1 c_{100}. \tag{12}$$

In the case where all collisions and evaporations are allowed, the formation rate must include all collisions which result in a cluster outside of the system. We tested that the boundary value $i_{\text{boundary}}$ was large enough so that an increase in the system size did not affect the results. We controlled the monomer concentration $c_1$, and in the ion-induced case also the concentration of ions, and kept track of the total concentration of molecules $c_{\text{tot}} = \sum_i i c_i$. We extracted the steady-state nucleation/formation rate at different vapour concentrations and studied the behaviour of the rate as a function of the vapour concentration. We then compared the predictions of Eqs. (6), (7), (9), and (10) to the simulation results.

The following physical properties of water were used (at $T = 273.15$ K): a molecular mass of 18.02 g/mol, a liquid density of 998.0 kg/m$^3$ (which was used to provide an estimate of the molecular volume), a surface tension of $\sigma = 0.075660$ N/m, and a saturated vapour pressure of 610.3 Pa.[34]

## III. RESULTS

### A. Homogeneous nucleation

Our simulations confirm that in the case of homogeneous one-component nucleation where there are no minima on the formation free energy versus cluster size curve (Fig. 1), both Eqs. (6) and (7) for the nucleation rate predict the simulation results accurately (see Fig. 2). Also, the slope of the $\ln J$ versus $\ln c_1$ curve gives the critical cluster size correctly, when

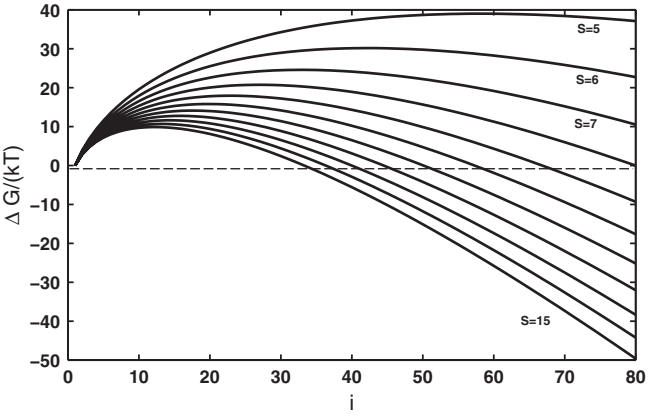


FIG. 1. The free energy profiles as a function of the number of molecules in the cluster for pure water at 273.15 K. The curves represent different saturation ratios, progressing from $S = 5$ (highest curve) to $S = 15$ (lowest curve) in increments of one saturation unit.

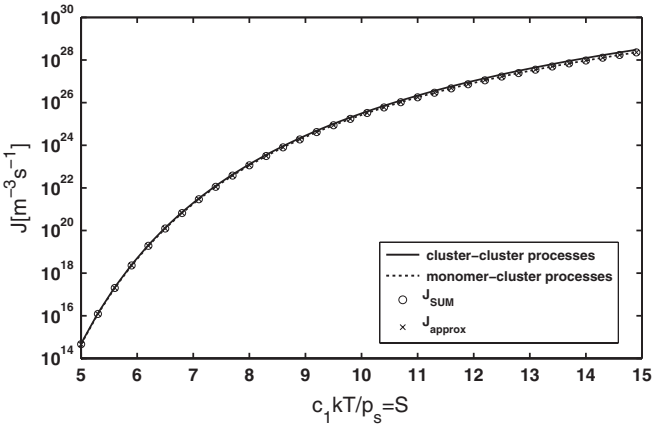


FIG. 2. The nucleation rates as a function of saturation ratio for pure water at $T = 273.15$ K obtained by explicit solution of the birth-death equations including all cluster-cluster collisions and evaporations (solid line) and only monomer collisions and evaporations (dashed line), the summation form of the nucleation rate Eq. (6) (circles) and the approximate form of the nucleation rate Eq. (7) (crosses).

the kinetic correction term $\epsilon = 1$ is taken into account (see Fig. 3). These are well-known results serving as a baseline for our study and confirming that our simulation method is working correctly. Allowing cluster-cluster collisions and evaporations or forbidding them did not make a significant difference, since the cluster distribution is dominated by the monomers, and the monomer concentration is a very good approximation of the total number $c_{\mathrm{tot}} = \sum_i i c_i$ of nucleating molecules in the system.

### B. Fictitious single component case with a free-energy minimum

Next, we studied a fictitious electrically neutral single component case. For collision coefficients the physical properties of water (at 273.15 K) were again used, but the free energy curves were artificially modified to contain a minimum between cluster sizes of 3 to 9 and a maximum at 10–

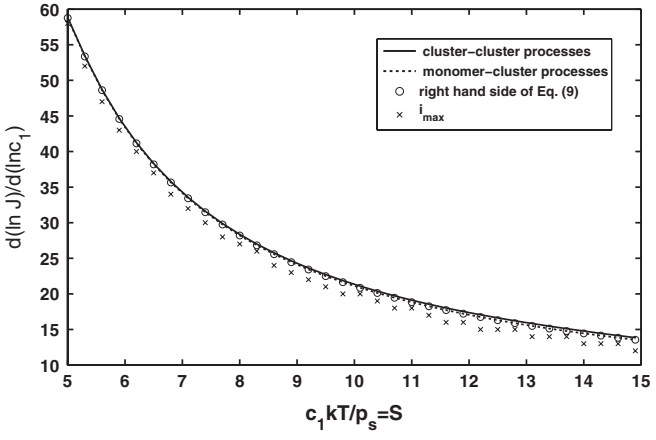


FIG. 3. The slope of the ln $J$ versus ln $c_1$ curve as a function of the saturation ratio for the homogeneous nucleation of pure water. The lines represent the values obtained from explicit solution of the birth-death equations including all cluster-cluster collisions and evaporations (solid) and only monomer collisions and evaporations (dashed). The circles represent the right hand side of Eq. (9), and the crosses give the location of the maximum in the free energy profile, which differ by $\epsilon = 1$ from the slope according to Eq. (10).

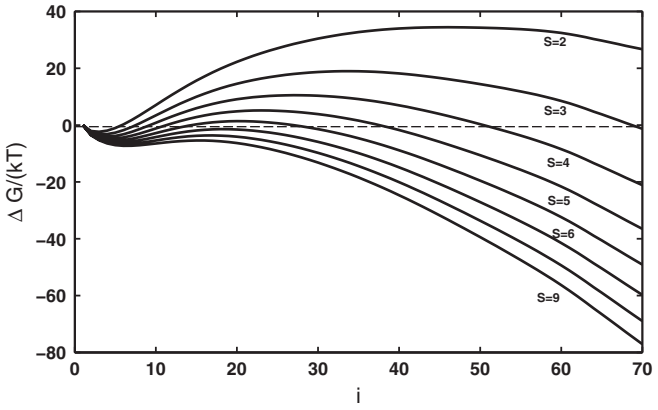


FIG. 4. The free energy profiles of the fictitious single component system explored in this work, as a function of the number of molecules in the cluster. The curves represent different saturation ratios, progressing from $S = 2$ (highest curve) to $S = 9$ (lowest curve) in increments of one saturation unit.

50 molecules. The resulting free energy curves are shown in Fig. 4 (numerical values are given in the Appendix). Note that when the saturation ratio exceeds 6, the maximum falls below zero. With these high saturation ratios, the formation process is not nucleation but barrierless kinetically controlled cluster formation. In these cases merging with a cluster of any size is energetically favourable for a monomer.

Now the free energy curve contains a local minimum, and thus the cluster distribution is no longer dominated by the monomers. Instead, the concentration of clusters corresponding to the minimum of the free energy profile is highest. Thus, excluding cluster-cluster collisions in the kinetics results in a significant underestimation of the nucleation rate. It must be stressed that allowing only monomer collisions and evaporations in this system is a purely hypothetical and unrealistic exercise. Figure 5 demonstrates the significance of cluster-cluster collisions by comparing the simulated nucleation rate in the fictitious system as a function of vapour concentration in a case where all cluster-cluster collisions are allowed (solid lines), to a case where only monomer-cluster collisions are allowed (dashed lines). The predictions of the summation

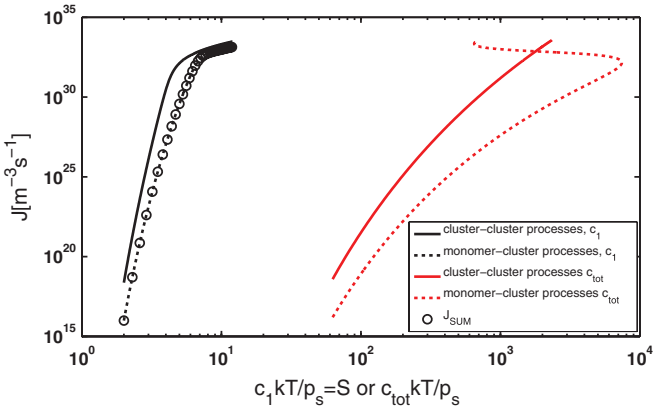


FIG. 5. The nucleation rates for the free energy profiles shown in Fig. 4. The $x$-axis shows either the saturation ratio $S = c_1 kT/p_s$ (black curves) or $c_{\mathrm{tot}} kT/p_s = \sum_i c_i kT/p_s$ (red curves). We allowed all collisions and evaporations (solid) or only monomer collisions and evaporations (dashed). Circles represent values calculated using the summation formula Eq. (6) for the nucleation rate.

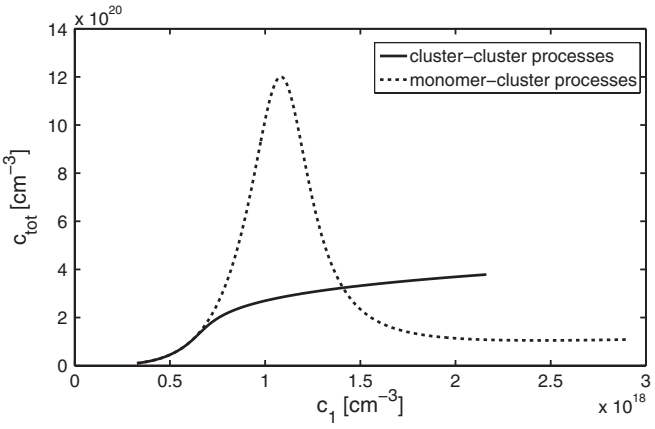


FIG. 6. The total concentration of vapour molecules versus the monomer concentration for the fictitious one-component system. Result for simulations allowing cluster-cluster processes and only monomer-cluster processes are shown.

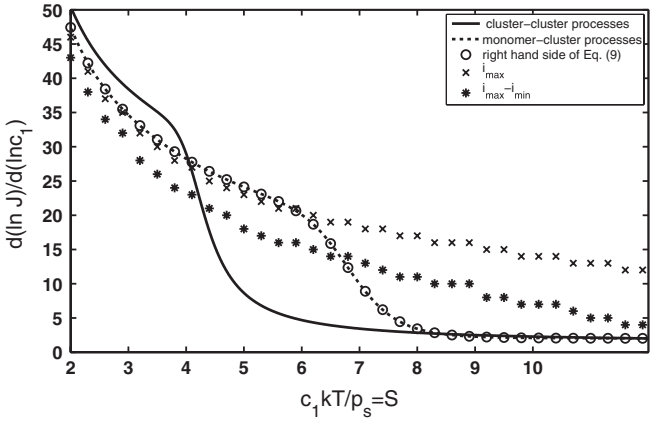


FIG. 7. The slope of the ln $J$ versus ln $c_1$ curve as a function of the saturation ratio $S = c_1 kT/p_s$ for the fictitious single component system of Fig. 4. We allowed only monomer collisions and evaporations (solid) or all collisions and evaporations (dashed). The circles refer to the right hand side of Eq. (9), the crosses to the value location of the free energy maximum $i_{\max}$ and the asterisks to the difference between the maximum and minimum $i_{\max} - i_{\min}$ (see discussion related to Fig. 10 concerning the latter.)

formula for the nucleation rate, Eq. (6), are shown as circles, demonstrating that the applicability of Eq. (6) (and the approximate rate Eq. (7) derived from Eq. (6)) is restricted to the case where monomer-cluster collisions dominate the kinetics. In the high saturation ratio region where the cluster formation is barrierless, the formation rates with and without cluster-cluster collisions merge, reflecting the fact that collision of two monomers is the crucial step under these conditions.

When monomers no longer dominate the total concentration of nucleating molecules in the system, the definition of the vapour concentration and its application involve some ambiguity. The saturation ratio is proportional to the number of monomers, $S = c_1 kT/p_s$, which is used as the $x$-axis for the black curves and symbols in Fig. 5. In experiments, the measured vapour concentration often contains the contribution of all small sizes, and the particle formation rate is plotted against $c_{\text{tot}} = \sum_i i c_i$.[25,35] The red curves in Fig. 5 demonstrate how the formation rate versus vapour concentration behaves if this practise is adopted. To shed light on the behaviour of the red curves in Fig. 5, Fig. 6 shows the total concentration of vapour molecules as a function of the monomer concentration in our simulations. In the fictional system described in this section, the total number of molecules can actually be approximated by the number of molecules in the cluster located at the minimum (for figure clarity, these results are not shown). The total molecular concentration does not depend on the monomer concentration linearly. Thus, the slope of ln $J$ as a function of ln $c_{\text{tot}}$ differs from the slope of ln $J$ as a function of ln $c_1$, and the nucleation theorem can not be safely applied to the $J$ vs $c_{\text{tot}}$ data. In the simulations allowing only monomer-cluster processes, $c_{\text{tot}}$ is not even a monotonous function of the monomer concentration. Thus, the same $c_{\text{tot}}$ can correspond to two different monomer concentrations and nucleation rates, explaining the strange behaviour of the dashed red line in Fig. 5.

Figure 7 shows the derivative of the formation rate as a function of $c_1 kT/p_s = S$. The dashed black line representing simulations with only monomer-cluster processes and the circles representing the right hand side of Eq. (9) agree well, as expected. An important observation is that in this case the nucleation theorem (Eq. (10)) is not valid: the crosses represent the location of the free energy maximum $i_{\max}$ and (even with a correction term $\epsilon = 1$) they do not match the dashed black curve at high saturation ratios. As mentioned before, deriving the approximate form of the theorem Eq. (10) from the general form Eq. (9) relies on significant values of exp $(-\Delta G/(kT))$ concentrating symmetrically around $i_{\max}$, and this is not valid for the free energy profiles seen in Fig. 4 when $S \geq 6$. The asterisks in Fig. 7 represent the difference $i_{\max} - i_{\min}$: the reasons for plotting this difference are discussed in Sec. III C. If either of the two restrictions (1) "monomer-cluster collisions and evaporations dominate" or (2) "the relevant (measured) vapour concentration is the concentration of monomers" is lifted, neither the critical cluster size $i_{\max}(+1)$ nor the right hand side of Eq. (9) agree with the slope of the nucleation rate. In the barrierless region above saturation ratio 6 all the simulation results eventually capture a slope of two, consistent with the kinetically controlled regime where cluster formation depends on the collision rate of two molecules. However, only the most realistic model, with cluster-cluster collisions and evaporations included (solid line) captures correctly the onset of the kinetic regime just above saturation ratio 6.

### C. Ion-induced nucleation of water

Ion-induced nucleation is an extensively studied case with a minimum in the free energy profile, and thus we explored the implications of our findings concerning the applicability of the nucleation theorem in this case. Figure 8 shows free energy profiles for the ion-induced nucleation of water with an ion radius of 1 Å. A major difference compared to the case described in Sec. III B is that the colliding vapour monomer is no longer on the one-dimensional free energy profile. The ions and vapour form, strictly speaking, a two-component system. The clusters depicted in Fig. 8 consist of one ion and $i$ water molecules, where $i$ can also be

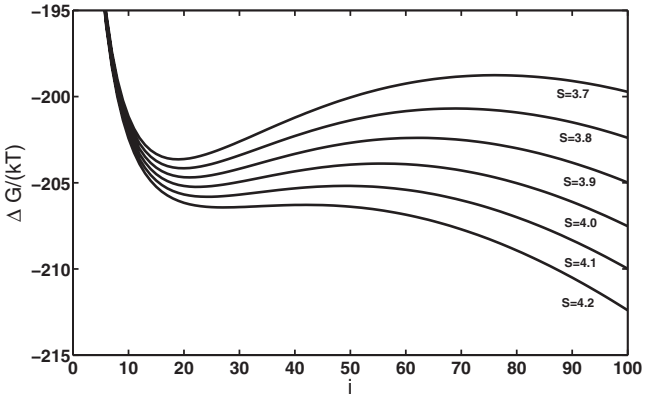


FIG. 8. The free energy profiles of ion-induced water nucleation on an ion with radius 1 Å at 273.15 K for various saturation ratios. Starting from the top curve, $S = 3.7$, 3.8, 3.9, 4.0, 4.1, and 4.2. The $x$-axis indicates the number of water molecules present in the cluster.

equal to zero. Ion-induced nucleation generally results in a significantly lower free energy barrier than the homogeneous vapour system (see Fig. 1), which means that the homogeneous vapour not containing any ions can be ignored in the ion-induced nucleation simulations. Importantly, due to electrostatic repulsion, it is unlikely that any clusters containing ions of the same sign will collide with each other to form new clusters. In this case, setting the monomer concentration to be much higher than that of ions, we have a system where cluster-cluster collisions can be ignored and the vapour concentration is equal to the number of monomers, while at the same time we have pre-nucleation clusters at the free energy minimum. Besides the temperature, there are now two parameters governing the system: the concentration of monomers (saturation ratio), and the concentration of ions.

Figure 9 shows the formation rate $J$ and Figure 10 the slope of the ln $J$ versus ln $S$ curve. Different results arise from different constraints for the ion concentration. The ion

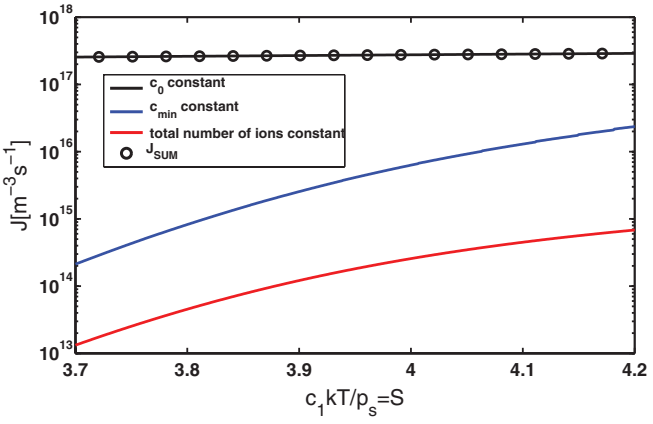


FIG. 9. The nucleation rates for the ion-induced free energy profiles shown in Fig. 8. The curves differ by the constraint applied to the ion concentration: the blue curve corresponds to setting the concentration of ions at the free energy minimum to $10^3$ cm$^{-3}$, the red curve setting the total concentration of ions to $10^3$ cm$^{-3}$, and the black curve setting the bare ion concentration to $10^3$ cm$^{-3}$. Circles represent values calculated using the summation form, Eq. (6), for the nucleation rate.

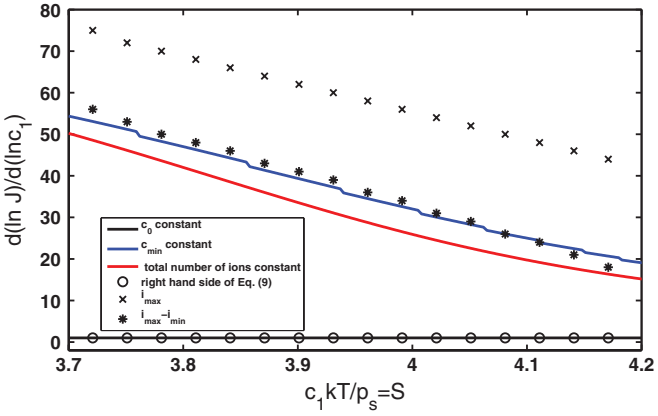


FIG. 10. The slope of the nucleation rate versus saturation ratio curve on a log-log scale as a function of the saturation ratio for ion-induced nucleation of water. The free energy profiles corresponding to this system are shown in Fig. 8. The curves differ by the constraint applied to the ion concentration: the blue curve corresponds to setting the concentration of ions at the free energy minimum to $10^3$ cm$^{-3}$, the red curve setting the total concentration of ions to $10^3$ cm$^{-3}$, and the black curve to setting the bare ion concentration to $10^3$ cm$^{-3}$. The circles refer to the right hand side of Eq. (9), the crosses to the values of the cluster size at the maximum ($i_{\max}$) and the asterisks to the difference between the maximum and minimum ($i_{\max} - i_{\min}$).

concentration value $10^3$ cm$^{-3}$ was selected because it is approximately the ion concentration in the atmosphere.[36] If the concentration of bare ions is kept constant at $10^3$ cm$^{-3}$ (when changing the water saturation ratio), the resulting ln $J$ − ln $c_1$ slope is always equal to one (black horizontal line). This reflects the fact that from the point of view of the water monomer, the whole free energy curve in Fig. 8 lies below zero, and the formation process is essentially a barrierless collision between the ion and the monomer, proportional to the first power of the ion concentration and the first power of water monomer concentration. The right hand side of Eq. (9) also predicts a slope of one (circles). A more realistic approach is to set the total number of ions ($\sum_i c_i$ instead of $\sum_i i c_i$ which is the total number of water molecules) or a closely related number of clusters (or ions) in the free energy minimum $c_{\min}$ constant (again at $10^3$ cm$^{-3}$), in which case the rate and the slope are given by the red and blue curves, respectively. Crosses denote the location of the free energy maximum $i_{\max}$, and asterisks represent the difference $i_{\max} - i_{\min}$. As expected from the classical form of nucleation rate in the ion-induced case[17]

$$J_{\text{ion-induced}} \propto \exp\left(\frac{-\Delta G_{\max} + \Delta G_{\min}}{kT}\right), \tag{13}$$

the difference $i_{\max} - i_{\min}$ gives the slope with a good accuracy in the case where the number of ions at the free energy minimum $c_{\min}$ is kept constant when changing the vapour concentration. We have indeed shown that this case is analogous to simulating homogeneous nucleation: we get the same results for the nucleation rate if we ignore equations describing cluster sizes $i < i_{\min}$, and start the simulations from $i = i_{\min}$ with the reference free energy shifted so that $\Delta G_{\min} = 0$. This results in free energy profiles similar to those in Fig. 1. The red curve in Fig. 10 shows that keeping the total number of ions constant does not result in quite the same slope

as in the case of the blue curve. Our results therefore highlight that the underlying assumption of the commonly used ion-induced nucleation theory is to fix the number of clusters (or ions) at the free energy minimum. Figure 7 shows that unlike in the ion-induced case, $i_{max} - i_{min}$ is not a good approximation of the slope in the fictitious one-component system, where cluster-cluster collisions and evaporations are at work. One could argue that rather than the total ion concentration, the production rate of ions is constant in the nature. In our model, which assumes time-independent steady-state nucleation and contains no other ion losses than the nucleation flow, the ion production rate is always necessarily equal to the steady-state nucleation rate. Studying the dependence of the nucleation rate on any parameter with the ion production rate held constant does, therefore, not result in informative correlations. We have used atmospheric ion concentrations and water as the nucleating vapour. The typical vapour concentration is therefore around 14 orders of magnitude higher than the ion concentration, and vapour molecules attached to ionic clusters can be completely neglected when calculating the total number of vapour molecules. In this case, there is no ambiguity in what is meant by the vapour concentration. In the atmosphere, where the actual nucleating vapour is a trace gas such as sulphuric acid with much lower concentrations, a significant or dominant part of the vapour molecules may be attached to ionic clusters. In such cases, the interpretation of the vapour concentration as either the total number of molecules or free monomers has similar consequences as seen in Sec. III B.

## IV. CONCLUSIONS

We have shown here that in a case where stable pre-nucleation clusters are formed, cluster-cluster collisions, and the possible contribution of clusters larger than monomers to the measured vapour concentration, distort the simple relation $d \ln J/d \ln c_{vapour} \approx i_{max}$. In ion-induced nucleation where cluster-cluster collisions can be neglected, the theorem can be applied in the form $d \ln J/d \ln c_{vapour} \approx i_{max} - i_{min}$ provided that the number of ions at the free energy minimum is kept constant. Without additional information about the existence of pre-nucleation clusters, correlations between the formation rate and the vapour concentration can not be used to deduce critical cluster properties.

Current scientific knowledge does not allow us to deduce the nature of the molecular mechanism governing atmospheric particle formation; the existence of small clusters in a free energy minimum is a possibility strongly suggested by experimental and theoretical evidence,[37–39] and must be kept in mind when analysing experimental data. When using theoretical chemistry to study clusters, we are often restricted to the smallest sizes. The dimer is a local minimum in one-component sulphuric acid nucleation, and quantum chemical studies predict local free energy minima in systems consisting of sulphuric acid, ammonia, dimethylamine, and water.[37] Due to the enormity of the numerical task we can not yet tell whether the maximum or the saddle point is below or above the reference level, indicating either barrierless cluster formation or nucleation involving stable pre-nucleation clusters, respectively.

Our results emphasise the importance of the choice of the reference size, which is the fundamental building block of the clusters, and whose concentration is controlled by processes other than particle formation, for example, by atmospheric gas-phase chemistry. If the reactions governing the formation of the reference size are much faster than particle formation, the reference size concentration will be constant throughout the formation event. In our simplistic model systems, the effect of the choice of the reference size is most dramatically manifested in the case of the ion-induced system, where the choice of a bare ion as the reference size results in a $\ln J$ versus $\ln c_{vapour}$ slope of one, whereas the choice of the cluster at the free energy minimum results in a slope $i_{max} - i_{min}$. For example, in particle formation involving sulphuric acid and some amine, the amine and sulphuric acid monomers are feasible choices as building blocks, but an equally justified choice may be the aminium bisulphate (1+1) cluster or aminium sulphate (1+2) cluster.

A slope between 1 and 2 in $\ln J$ versus $\ln c_{H_2SO_4}$ plots has been observed in many field and laboratory studies related to atmospheric particle formation.[7–9] Based on application of the nucleation theorem, this has been taken to indicate that the critical clusters in atmospheric nucleation contain 1 or 2 sulphuric acid molecules. While in our simple fictitious one-component system, this would be interpreted as barrierless cluster formation, in a process analogous to the ion-induced case in our study it could result from nucleation with any $i_{max} - i_{min} = 1 - 2$. For example, Köhler-type processes,[40] where vapour is condensing on a soluble seed, exhibit a minimum followed by a maximum in the free energy profiles as a function of the condensing vapour concentration and the seed concentration as a control parameter similar to the concentration of ions. Such a case can correspond to our simple ion-induced model or to the fictitious one-component system, or a hybrid of them, depending on the relative concentrations of the species involved. Thus, we should not limit ourselves to studying clusters with only 1 or 2 sulphuric acid molecules when looking for the key players in atmospheric particle formation.

## ACKNOWLEDGMENTS

We thank Joonas Merikanto, Madis Noppel, Ilona Riipinen, and Mikko Sipilä for useful discussions. We acknowledge the Academy of Finland (Project No. 1127372, Center of Excellence program Project No. 1118615, LASTU program Project No. 135054), ERC Project Nos. 257360-MOCAPAF and 27463-ATMNUCLE and NSF Grant No. OISE-0853294 for funding.

## APPENDIX: FREE ENERGY PROFILE FOR THE NEUTRAL ONE-COMPONENT SYSTEM

For the fictitious neutral one-component system, the free energy profile is given in Table I for $S = 1.0$, and was generated by hand with some numerical smoothing techniques to give the behaviour described in the text. The

TABLE I. The formation free energy profile for the fictitious one-component system as a function of cluster size at saturation ratio $S = 1$.

| $i$ | $\Delta G/k_bT$ | $i$ | $\Delta G/k_bT$ | $i$ | $\Delta G/k_bT$ |
|---|---|---|---|---|---|
| 1 | 0.0000000 | 25 | 43.6602058 | 48 | 66.9640503 |
| 2 | − 1.3922136 | 26 | 45.1312637 | 49 | 67.6142120 |
| 3 | − 0.9622458 | 27 | 46.5517654 | 50 | 68.2491684 |
| 4 | 0.1332060 | 28 | 47.9239960 | 51 | 68.8690414 |
| 5 | 1.7300825 | 29 | 49.2497253 | 52 | 69.4731140 |
| 6 | 3.6929119 | 30 | 50.5302887 | 53 | 70.0596771 |
| 7 | 5.9110312 | 31 | 51.7666664 | 54 | 70.6260300 |
| 8 | 8.2951708 | 32 | 52.9595757 | 55 | 71.1683731 |
| 9 | 10.7743788 | 33 | 54.1095963 | 56 | 71.6818542 |
| 10 | 13.2932558 | 34 | 55.2172394 | 57 | 72.1606293 |
| 11 | 15.8094959 | 35 | 56.2830696 | 58 | 72.5979767 |
| 12 | 18.2916965 | 36 | 57.3077660 | 59 | 72.9865036 |
| 13 | 20.7174244 | 37 | 58.2922096 | 60 | 73.3184509 |
| 14 | 23.0715237 | 38 | 59.2375298 | 61 | 73.5860596 |
| 15 | 25.3446426 | 39 | 60.1451187 | 62 | 73.7820969 |
| 16 | 27.5319462 | 40 | 61.0166817 | 63 | 73.9004822 |
| 17 | 29.6320496 | 41 | 61.8541908 | 64 | 73.9370575 |
| 18 | 31.6460724 | 42 | 62.6598740 | 65 | 74.0905075 |
| 19 | 33.5768852 | 43 | 63.4361496 | 66 | 74.1635056 |
| 20 | 35.4284706 | 44 | 64.1855621 | 67 | 74.2639389 |
| 21 | 37.2054214 | 45 | 64.9106827 | 68 | 74.3064651 |
| 22 | 38.9125328 | 46 | 65.6139984 | 69 | 74.4141998 |
| 23 | 40.5545158 | 47 | 66.2978058 | 70 | 74.5207062 |
| 24 | 42.1357574 | | | | |

conversion to other saturation ratios is given by

$$\Delta G(i) = \Delta G_{S=1}(i) - (i-1)kT \times \ln S, \tag{A1}$$

where $i$ is the size of the cluster.


[1] M. Kulmala, H. Vehkamäki, T. Petäjä, M. Dal Maso, A. Lauri, V.-M. Kerminen, W. Birmili, and P. H. McMurry, J. Aerosol Sci. **35**, 143 (2004).
[2] D. V. Spracklen, K. S. Carslaw, M. Kulmala, V.-M. Kerminen, S.-L. Sihto, I. Riipinen, J. Merikanto, G. W. Mann, M. P. Chipperfield, A. Wiedensohler, W. Birmili, and H. Lihavainen, Geophys. Res. Lett. **35**, L06808, doi:10.1029/2007GL033038 (2008).
[3] J. Merikanto, D. V. Spracklen, G. W. Mann, S. J. Pickering, and K. S. Carslaw, Atmos. Chem. Phys. **9**, 8601 (2009).
[4] J. Kazil, P. Stier, K. Zhang, J. Quaas, S. Kinne, D. O'Donnell, S. Rast, M. Esch, S. Ferrachat, U. Lohmann, and J. Feichter, Atmos. Chem. Phys. Discuss. **10**, 12261 (2010).
[5] R. J. Weber, J. Marti, P. H. McMurry, F. L. Eisele, D. J. Tanner, and A. Jefferson, Chem. Eng. Commun. **151**, 53 (1996).
[6] M. Kulmala, K. E. J. Lehtinen, and A. Laaksonen, Atmos. Chem. Phys. **6**, 787 (2006).
[7] S.-L. Sihto, M. Kulmala, V.-M. Kerminen, M. Dal Maso, T. Petäjä, I. Riipinen, H. Korhonen, F. Arnold, R. Janson, M. Boy, A. Laaksonen, and K. E. J. Lehtinen, Atmos. Chem. Phys. **6**, 4079 (2006).
[8] C. Kuang, P. H. McMurry, A. V. McCormick, and F. L. Eisele, J. Geophys. Res., [Atmos.] **113**, D10209, doi:10.1029/2007JD009253 (2008).
[9] M. Sipilä, T. Berndt, T. Petäjä, D. Brus, J. Vanhanen, F. Stratmann, J. Patokoski, R. L. Mauldin III, A.-P. Hyvärinen, H. Lihavainen, and M. Kulmala, Science **327**, 1243 (2010).
[10] S. M. Ball, D. R. Hanson, F. L. Eisele, and P. McMurry, J. Geophys. Res. D **104**, 23709, doi:10.1029/1999JD900411 (1999).
[11] A. Metzger, B. Verheggen, J. Dommen, J. Duplissy, A. S. H. Prevot, E. Weingartner, I. Riipinen, M. Kulmala, D. V. Spracklen, K. S. Carslaw, and U. Baltensperger, Proc. Natl. Acad. Sci. U.S.A. **107**, 6646 (2010).
[12] L. H. Young, D. R. Benson, F. R. Kameel, J. R. Pierce, H. Junninen, M. Kulmala, and S.-H. Lee, Atmos. Chem. Phys. **8**, 4997 (2008).
[13] D. R. Benson, L.-H. Young, F. R. Kameel, and S.-H. Lee, Geophys. Res. Lett. **35**, L11801, doi:10.1029/2008GL033387 (2008).
[14] D. Kashchiev, J. Chem. Phys. **76**, 5098 (1982).
[15] D. W. Oxtoby and D. Kashchiev, J. Chem. Phys. **100**, 7665 (1994).
[16] I. J. Ford, J. Chem. Phys. **105**, 8324 (1996).
[17] D. Kashchiev, *Nucleation: Basic Theory with Applications* (Butterworths, Oxford, 2000).
[18] J. L. Katz, H. Saltsburg, and H. Reiss, J. Colloid Interface Sci. **21**, 560 (1966).
[19] R. H. Heist, K. M. Colling, and C. S. DuPuis, J. Chem. Phys. **65**, 5147 (1976).
[20] Y. G. Russell and R. H. Heist, J. Chem. Phys. **69**, 3723 (1978).
[21] G. Agarwal and R. H. Heist, J. Chem. Phys. **73**, 902 (1980).
[22] H. Reiss, J. Chem. Phys. **18**, 840 (1950).
[23] D. Stauffer, J. Aerosol Sci. **7**, 319 (1976).
[24] H. Vehkamäki, *Classical Nucleation Theory in Multicomponent Systems* (Springer, Berlin, 2006).
[25] M. Noppel, H. Vehkamäki, and M. Kulmala, J. Chem. Phys. **116**, 218 (2002).
[26] F. F. Abraham, *Homogeneous Nucleation Theory* (Academic, New York, 1974).
[27] J. Frenkel, J. Chem. Phys. **7**, 538 (1939).
[28] R. McGraw and D. T. Wu, J. Chem. Phys. **118**, 9337 (2003).
[29] R. McGraw and R. Zhang, J. Chem. Phys. **128**, 064508 (2008).
[30] H. Vehkamäki, A. Määttänen, A. Lauri, and M. Kulmala, J. Chem. Phys. **126**, 174707 (2007).
[31] P. M. Winkler, G. Steiner, A. Vrtala, H. Vehkamäki, M. Noppel, K. E. J. Lehtinen, G. P. Reischl, P. E. Wagner, and M. Kulmala, Science **319**, 1374 (2008).
[32] M. Kulmala, G. Mordas, T. Petäjä, T. Grönholm, P. P. Aalto, H. Vehkamäki, A. I. Hienola, E. Herrmann, M. Sipilä, I. Riipinen, H. E. Manninen, K. Hämeri, F. Stratmann, M. Bilde, P. M. Winkler, W. Birmili, and P. E. Wagner, J. Aerosol Sci. **38**, 289 (2007).
[33] M. J. McGrath, T. Olenius, I. K. Ortega, V. Loukonen, P. Paasonen, T. Kurtén, M. Kulmala, and H. Vehkamäki, Atmos. Chem. Phys. Discuss. **11**, 25263 (2011).
[34] *NIST Chemistry WebBook*, NIST Standard Reference Database Vol. 69, edited by P. J. Linstrom and W. G. Mallard (National Institute of Standards and Technology, Gaithersburg, Maryland, 2011); see http://webbook.nist.gov.
[35] A. Jaecker-Voirol, P. Mirabel, and H. Reiss, J. Chem. Phys. **87**, 4849 (1987).
[36] H. E. Manninen, T. Nieminen, E. Asmi, S Gagné, S. Häkkinen, K. Lehtipalo, P. P. Aalto, M. Vana, A. Mirme, S. Mirme, U. Hõrrak, C. Plass-Dülmer, G. Stange, G. Kiss, A. Hoffer, A. N. Törő, M. Moerman, B. Henzing, G. de Leeuw, M. Brinkenberg, G. N. Kouvarakis, A. Bougiatioti, N. Mihalopoulos, C. O'Dowd, D. Ceburnis, D. A. Arneth, B. Svenningsson, E. Swietlicki, L. Tarozzi, S. Decesari, M. C. Facchini, W. Birmili, A. Sonntag, A. Wiedensohler, J. Boulon, K. Sellegri, P. Laj, M. Gysel, N. Bukowiecki, N. E. Weingartner, G. Wehrle, A. Laaksonen, A. Hamed, J. Joutsensaari, T. Petäjä, V.-M. Kerminen, and M. Kulmala, Atmos. Chem. Phys. **10**, 7907 (2010).
[37] I. K. Ortega, O. Kupiainen, T. Kurtén, T. Olenius, O. Wilkman, M. J. McGrath, V. Loukonen, and H. Vehkamäki, Atmos. Chem. Phys. **12**, 225 (2012).
[38] K. Lehtipalo, M. Sipilä, I. Riipinen, T. Nieminen, and M. Kulmala, Atmos. Chem. Phys. **9**, 4177 (2009).
[39] K. Lehtipalo, M. Kulmala, M. Sipilä, T. Petäjä, M. Vana, D. Ceburnis, R. Dupuy, and C. O'Dowd, Atmos. Chem. Phys. **10**, 7009 (2010).
[40] H. Köhler, Trans. Faraday Soc. **32**, 1152 (1936).